LETTERS

# Quantum oscillations in an overdoped high-$T_c$ superconductor

B. Vignolle[1], A. Carrington[2], R. A. Cooper[2], M. M. J. French[2], A. P. Mackenzie[3], C. Jaudet[1], D. Vignolles[1], Cyril Proust[1] & N. E. Hussey[2]

**The nature of the metallic phase in the high-transition-temperature (high-$T_c$) copper oxide superconductors, and its evolution with carrier concentration, has been a long-standing mystery[1]. A central question is how coherent electronic states, or quasiparticles, emerge from the antiferromagnetic insulator with doping. Recent quantum oscillation experiments on lightly doped copper oxides have shown evidence for small pockets of Fermi surface[2–5], the formation of which has been associated with the opening of the pseudogap—an anisotropic gap in the normal state excitation spectrum of unknown origin[1]. As the doping is increased, experiments suggest that the full Fermi surface is restored[6,7], although the doping level at which the pseudogap closes and the nature of the electronic ground state beyond this point have yet to be determined. Here we report the observation of quantum oscillations in the overdoped superconductor $Tl_2Ba_2CuO_{6+\delta}$ that show the existence of a large Fermi surface of well-defined quasiparticles covering two-thirds of the Brillouin zone. These measurements confirm that, in overdoped superconducting copper oxides, coherence is established at all Fermi wavevectors, even near the zone boundary where the pseudogap is maximal and electronic interactions are strongest; they also firmly establish the applicability of a generalized Fermi-liquid picture on the overdoped side of the superconducting phase diagram.**

According to density functional theory (DFT) band structure calculations for hole-doped copper oxides, the electronic states within the $CuO_2$ planes form a large, almost cylindrical Fermi surface comprising $1 + p$ quasiparticles, where $p$ is the number of doped holes per planar Cu ion[8,9]. In underdoped copper oxides, however, this band picture fails spectacularly owing to strong electron correlations and the opening of the pseudogap that depletes states in a manner yet to be fully understood[1]. Recently, small Fermi surface pockets were discovered in the underdoped yttrium-based copper oxides $YBa_2Cu_3O_{6.5}$ and $YBa_2Cu_4O_8$ through a series of quantum oscillation experiments[2–5]. In line with other bulk measurements, the area of these pockets was found to scale roughly with $p$, rather than $1 + p$, though neither their number nor their location are currently known. In marked contrast, angle-resolved photoemission spectroscopy (ARPES) measurements performed on other underdoped copper oxides suggest that the large underlying Fermi surface disintegrates into a set of disconnected Fermi arcs, centred on the zone diagonal, whose width diminishes with decreasing $p$ and temperature $T$ (ref. 10). This apparent disparity between the two experimental probes has yet to be resolved.

For heavily doped copper oxides, the situation is altogether different. Both interlayer angle-dependent magnetoresistance (ADMR)[6] and ARPES[7] measurements reveal a large quasi-two-dimensional Fermi surface in the single $CuO_2$ layer material $Tl_2Ba_2CuO_{6+\delta}$ (Tl2201), in broad agreement with DFT calculations[9] and earlier estimates from the low-temperature Hall coefficient[11]. Although ADMR is a useful probe of the underlying Fermi surface topology, it is a semi-classical effect and, as such, cannot give any definitive conclusions about the quantum mechanical nature of the electronic ground state. Similarly, although quasiparticle-like peaks have been seen in the ARPES-derived energy-density curves around the full Fermi surface of overdoped copper oxides[7,12], their widths near the zone boundaries are often too broad (up to 0.1 eV) to be considered as conclusive evidence for the long-lived fermionic quasiparticle states predicted by DFT.

From this standpoint, the observation of quantum oscillations is a much more powerful, definitive signature of coherent quasiparticles. Quantum oscillations are periodic oscillations in bulk physical properties—for example in the magnetoresistance (the Shubnikov–de Haas effect) or the magnetization (the de Haas–van Alphen (dHvA) effect)—that arise from the magnetic-field-induced quantization of the allowed energy levels of the quasiparticles. The quantization condition that underlies this effect requires the quasiparticle wavefunction to remain coherent throughout an entire orbit of the Fermi surface, and hence the observation of quantum oscillations is a crucial test of the fermionic nature of the low-lying electronic states.

The difficulty of observing quantum oscillations in a metal with a large Fermi surface should not be underestimated. The ADMR/ARPES measurements described above imply the existence of a Fermi surface sheet in Tl2201 with an average Fermi wavevector $k_F$ a factor of six larger than that of the pocket first discovered in the yttrium-based copper oxides. The amplitude of the quantum oscillations is suppressed by impurity scattering as $\exp(-\pi\hbar k_F/eBl)$, where $e$ is the electronic charge and $l$ is the quasiparticle mean-free-path. At the combination of $B$ and $l$ (respectively 35 T and 165 Å) at which dHvA oscillations from the small Fermi surface first become visible in $YBa_2Cu_3O_{6.5}$ (ref. 5), the signal from a correspondingly large sheet would be damped by a further ten orders of magnitude. So for any experiment on overdoped copper oxides to be viable, it is essential to work at the highest magnetic fields, with optimized signal-to-noise ratio, on single crystals of the highest quality available.

The Tl2201 crystals used in this experiment (typical dimensions $0.2 \times 0.1 \times 0.02\,mm^3$) were grown via a self-flux method as described previously[13] and annealed in flowing oxygen at temperatures ranging from 270 °C to 450 °C for up one week in order to achieve a range of $T_c$ values between 10 K and 30 K. Around 20 crystals were then screened for purity by measuring their zero-field interlayer resistivity $\rho_\perp(T)$ with a four-terminal a.c. method. Only four crystals with sufficiently large residual resistivity ratios (~20) were selected for the high-field magnetoresistance measurements

[1]Laboratoire National des Champs Magnétiques Pulsés (LNCMP), UMR CNRS-UPS-INSA 5147, Toulouse 31400, France. [2]H. H. Wills Physics Laboratory, University of Bristol, Tyndall Avenue, Bristol BS8 1TL, UK. [3]Scottish Universities Physics Alliance, School of Physics and Astronomy, University of St Andrews, St Andrews, Fife KY16 9SS, UK.

carried out in a standard $^4$He cryostat at the LNCMP pulsed field facility in Toulouse using the same contact configuration. For the torque measurements, small pieces of the same crystals were attached to sensitive piezoresistive cantilevers and mounted in a dilution refrigerator in a second magnet cell at LNCMP.

Figure 1a, b shows interlayer resistance ($R_\perp$) data and magnetic torque ($\tau$) data with the field oriented close to the $c$ axis for two different Tl2201 crystals at temperatures below their zero-field superconducting transitions ($T_c \approx 10$ K). For both sets of data, an expanded view near the field maxima reveals clear oscillations whose amplitude grows with increasing field strength. Figure 1c shows the oscillatory part of the magnetization $\Delta\tau/B$ plotted versus inverse magnetic field $1/B$. The observation of oscillations, periodic in $1/B$, in both the magnetization and the resistivity, at fields well above the upper critical field $B_{c2}$, confirm these as quantum oscillations. Strikingly, as shown in Fig. 1c, these oscillations are more than one order of magnitude faster than those found in underdoped $YBa_2Cu_4O_8$.

The frequency ($F$) of the oscillations is directly related to the extremal cross-sectional area $A$ of the Fermi surface normal to the field orientation, via the Onsager relation, $A = 2\pi eF/\hbar$. Figure 2a shows the fast Fourier transform of the data in Fig. 1c. A single, sharp dHvA frequency of $18{,}100 \pm 50$ T is obtained, corresponding to a Fermi surface extremal cross-sectional area $A$ of $172.8 \pm 0.5$ nm$^{-2}$ and average $k_F$ of $7.42 \pm 0.05$ nm$^{-1}$. The temperature dependence of the Shubnikov–de Haas amplitude is shown in Fig. 2b. Fitting this with the standard Lifshitz–Kosevich theory, we obtain a cyclotron effective mass $m^* = 4.1 \pm 1.0\, m_e$, where $m_e$ is the free electron mass. Finally, Fig. 2c shows that the field dependence of the amplitude of the dHvA oscillations follows the expected exponential decay, from which we estimate $l = 320$ Å.

All these numbers are in excellent agreement with those deduced from other measurements in the same material with similar doping levels. The Fermi surface topology deduced from ADMR[6,14] is reproduced as a solid black line in Fig. 2a inset. Its area agrees extremely well with the measured dHvA frequency, and corresponds to ~65% of the Brillouin zone of Tl2201 and a doping level $p = 0.30$. In addition, given that for a two-dimensional Fermi surface, the electronic specific heat (Sommerfeld coefficient) is $\gamma_{el} = (\pi N_A k_B^2 a^2/3\hbar^2)m^*$ (where $k_B$ is the Boltzmann constant, $N_A$ is Avogadro's number, and $a = 3.86$ Å is the in-plane lattice constant[15]), our value of $m^*$ corresponds to $\gamma_{el} \approx 6.0 \pm 1.0$ mJ mol$^{-1}$ K$^{-2}$, in excellent agreement with that measured directly[16] for overdoped polycrystalline Tl2201 ($7 \pm 2$ mJ mol$^{-1}$ K$^{-2}$). Hence, in contrast to the previous work[2–5], we can make quantitative comparisons between quasiparticle properties derived from quantum oscillations at high fields and those measured directly by transport and thermodynamics at zero field. This good overall consistency suggests that the Fermi surface is composed entirely of the single quasi-two-dimensional sheet that we observe. DFT calculations predict that the bare band mass in stoichiometric Tl2201 is ~$1.2m_e$ (ref. 9). The difference between the measured and calculated masses implies strong electron-correlation-driven renormalization, even at this elevated doping level.

Despite strong electron–electron interactions, the observation of quantum oscillations implies that quasiparticles exist at all points on the Fermi surface of overdoped Tl2201. The observation of genuine quantum oscillations in Tl2201 supports the recognized idea that generalized Fermi-liquid theory can be applied on the overdoped side of the phase diagram. Moreover, the observation of quantum oscillations on both sides of optimal doping, albeit with very different frequencies, suggests that the quantum oscillations observed in underdoped copper oxides directly probe the Fermi surface there, rather than some anomalous vortex physics[17], and raises the intriguing prospect that quasiparticle states may survive, at least at some loci on the Fermi surface, across the entire doping range, from the insulating/superconducting boundary to the non-superconducting metal on the heavily overdoped side.

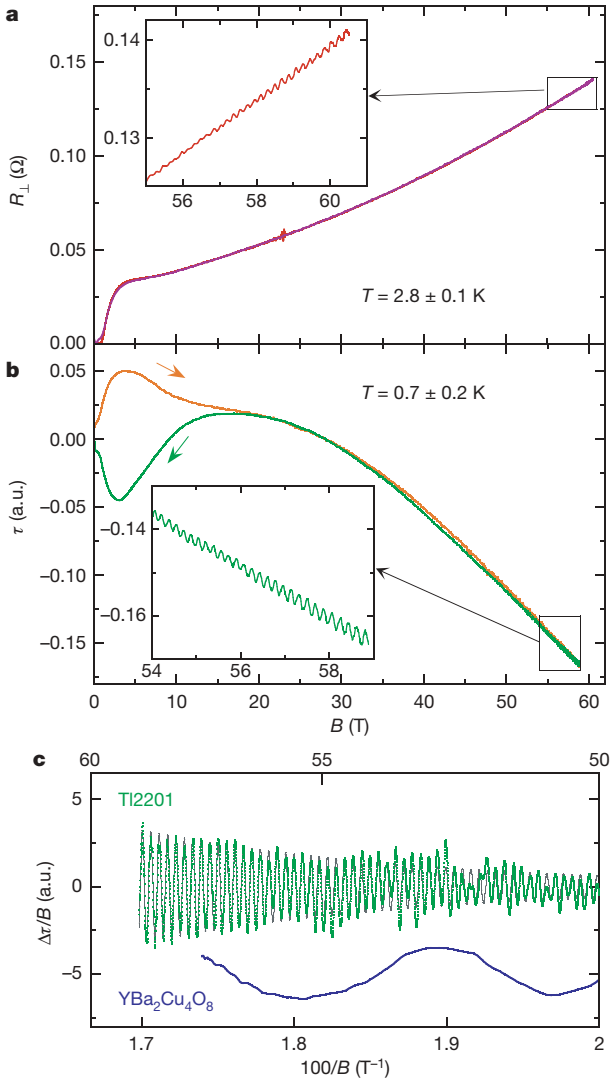


**Figure 1 | Quantum oscillations in Tl2201.** **a**, Raw data on interlayer resistance ($R_\perp$) with **B**//$c$ for a Tl2201 single crystal at $T = 2.8 \pm 0.1$ K. $R_\perp(B)$ rises rapidly above the irreversibility field $B_{irr}$, passes through a small plateau, then grows quasi-quadratically with field up to 60 T. Inset, magnified view of the high-field region of the down sweep. Small but well-defined oscillations are clearly resolved in the raw data, with an amplitude that grows with increasing field strength. The maximum amplitude of the oscillations is only 0.5 mΩ. **b**, Averaged magnetic torque data (from five sweeps at temperatures between 0.6 K and 0.8 K) with **B** close to the $c$ axis for a different Tl2201 crystal. The temperatures of the torque sweeps are subject to an additional uncertainty of 150 mK due to the weak thermal link inside the dilution refrigerator[5] and the high currents needed to observe the oscillations. Below $B = 14$ T, the torque shows hysteretic behaviour due to flux trapping and expulsion in the superconducting mixed state. Again, well-defined oscillations are clearly resolved in the expanded region shown in the inset. The value of $T_c$ for both crystals is 10 K (defined by their zero-resistive state), compared with the maximal $T_c$ in Tl2201 of 92 K. The torque crystal showed a very small kink in the zero-field $\rho_\perp$ data around 20 K, suggesting that some fraction of the crystal, presumably the surface layer, had a higher $T_c$ value. Note that the difference in $B_{irr}$ exhibited by both crystals is amplified in the pulsed magnetic field because the sweep rate d$B$/d$t$ for the higher $B_{irr}$ sample is greater. a.u., arbitrary units. **c**, The oscillatory component of the torque data shown in **b** plotted as green dots against $1/B$ (the corresponding $B$ values are shown at the top of the panel), after a monotonic background has been subtracted. The black line superimposed on the data is a fit to the Lifshitz–Kosevich expression for dHvA oscillations in a two-dimensional metal[29]. Also shown (blue), for comparison, is the oscillatory component in the torque signal on underdoped $YBa_2Cu_4O_8$.

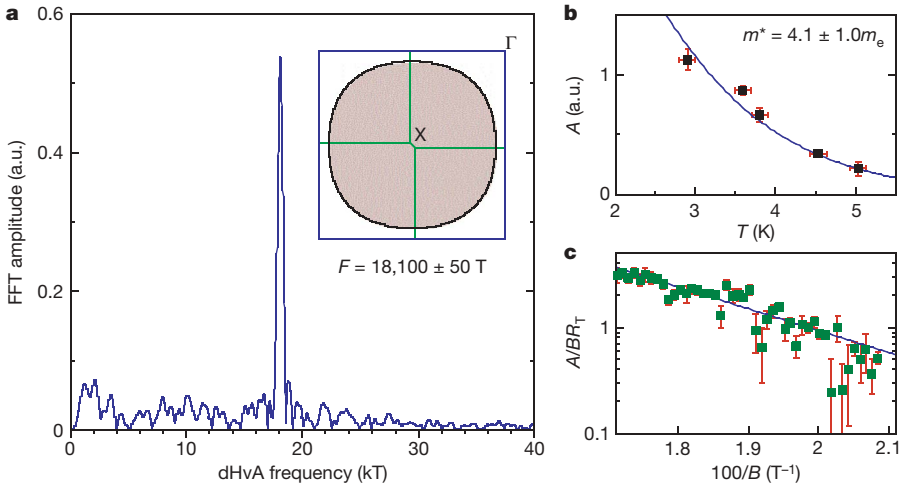


**Figure 2 | Features of the oscillation data. a**, Fast Fourier transform (FFT) of the data shown in Fig. 1c (field range 50–58.8 T), revealing a single, sharp dHvA frequency of $F = 18{,}100 \pm 50$ T, corresponding to an average Fermi surface radius $k_F = 7.42 \pm 0.05$ nm$^{-1}$. Inset, a cross-section of the Fermi surface topology of overdoped Tl2201 ($T_c = 15$ K) deduced from ADMR[6,14]. The area of this tubular Fermi surface is in excellent agreement with our measured dHvA frequency. **b**, Temperature dependence of the Shubnikov–de Haas amplitude. According to the standard Lifshitz–Kosevich expression for the oscillatory magnetization[29], the thermal damping factor $R_T = X/\sinh(X)$, where $X = (2\pi^2 k_B/\hbar e)m^*T/B$ and $m^*$ is the quasiparticle effective mass that is enhanced over the band-mass by many-body interactions. Error bars, $1\sigma$. **c**, Field dependence of the amplitude of the dHvA oscillations shown in Fig. 1c, divided by $R_T$. Each point represents a fit of 1.5 oscillations to $A/(R_T B)\sin(2\pi F/B + \phi)$. From the fit to the exponential decay, we tentatively estimate a mean-free-path of $l = 320$ Å. The actual mean-free-path may be up to a factor of two longer than this, because the limited field range of our measurements does not allow us to rule out a low frequency beat with another close frequency, as expected for a quasi-two-dimensional Fermi surface such as this[30]. The transport mean-free-path in the best crystals, as estimated from in-plane resistivity measurements[11], is of the order $l = 670$ Å. Error bars are deduced from a combination of systematic error and standard deviation.

Another noteworthy feature of this result is that quantum oscillations have been observed in a metal for which one key signature of a Landau Fermi-liquid, namely a purely quadratic temperature dependence of the electrical resistivity at low temperatures, is absent. According to ADMR experiments on overdoped Tl2201 crystals with comparable $T_c$ values, the scattering rate contains two temperature-dependent components; a dominant isotropic component, which varies quadratically with temperature and is characteristic of fermionic quasiparticle scattering, and an anisotropic component, maximal near the Brillouin zone boundaries and varying linearly with temperature down to very low temperatures[14], consistent with the observed form of the in-plane resistivity[11,18]. This unusual form of the scattering rate has been associated with proximity to a quantum critical point[19,20] or to the Mott insulating state[21], but its origin is as yet unknown. The fact that quasiparticles arise, despite there being a linear-in-$T$ contribution to the scattering rate, is in agreement with theoretical predictions[22,23]. However, to actually see the effect of the anomalous contribution to the self energy in the temperature dependence of the oscillations would require following them to much lower temperature[23,24].

Finally, our measurements offer strong support for the scenario[25] that beyond a critical doping level within the superconducting dome, the pseudogap vanishes—that is, that the pseudogap and the superconducting gap are not coincident in the overdoped regime. We stress here that closure of the pseudogap is not field-induced, as the Fermi surface parameters we derive are entirely consistent with zero-field transport[11], thermodynamic[17] and spectroscopic[7] data. The task now is to determine whether this large Fermi surface evolves into a collection of small pockets or into a series of disconnected arcs at low doping. In other words, does the carrier density decrease smoothly from $1 + p$ to $p$, or does a competing order—such as antiferromagnetism[26], $d$-density-wave[27], orbital loops[20] or stripes[28]—cause a Fermi surface reconstruction along some critical line in the ($p$, $T$) phase diagram? Given the excellent agreement between dHvA and ARPES results evident in overdoped Tl2201, combined measurements on the same underdoped compound seem to be essential to help resolve this long-standing controversy.

**Received 4 June; accepted 28 July 2008.**


1. Timusk, T. & Statt, B. The pseudogap in high temperature superconductors: An experimental survey. *Rep. Prog. Phys.* **62**, 61–122 (2000).
2. Doiron-Leyraud, N. *et al.* Quantum oscillations and the Fermi surface in an underdoped high-$T_c$ superconductor. *Nature* **447**, 565–568 (2007).
3. Yelland, E. A. *et al.* Quantum oscillations in the underdoped cuprate $YBa_2Cu_4O_8$. *Phys. Rev. Lett.* **100**, 047003 (2008).
4. Bangura, A. F. *et al.* Small Fermi surface pockets in underdoped high temperature superconductors: Observation of Shubnikov-de Haas oscillations in $YBa_2Cu_4O_8$. *Phys. Rev. Lett.* **100**, 047004 (2008).
5. Jaudet, C. *et al.* de Haas–van Alphen oscillations in the underdoped high-temperature superconductor $YBa_2Cu_3O_{6.5}$. *Phys. Rev. Lett.* **100**, 187005 (2008).
6. Hussey, N. E. *et al.* A coherent three-dimensional Fermi surface in a high transition temperature superconductor. *Nature* **425**, 814–817 (2003).
7. Platé, M. *et al.* Fermi surface and quasiparticle excitations of overdoped $Tl_2Ba_2CuO_{6+\delta}$. *Phys. Rev. Lett.* **95**, 077001 (2005).
8. Andersen, O. K., Liechtenstein, A. I., Jepsen, O. & Paulsen, F. LDA energy bands, low energy Hamiltonians, $t'$, $t''$, $t_\perp(\mathbf{k})$ and $J_\perp$. *J. Phys. Chem. Solids* **56**, 1573–1591 (1995).
9. Singh, D. J. & Pickett, W. E. Electronic characteristics of $Tl_2Ba_2CuO_6$. *Physica C* **203**, 193–199 (1992).
10. Kanigel, A. *et al.* Evolution of the pseudogap from Fermi arcs to the nodal metal. *Nature Phys.* **2**, 447 (2006).
11. Mackenzie, A. P., Julian, S. R., Sinclair, D. C. & Lin, C. T. Normal state magnetotransport in superconducting $Tl_2Ba_2CuO_{6+\delta}$ to millikelvin temperatures. *Phys. Rev. B* **53**, 5848–5854 (1996).
12. Yusof, Z. M. *et al.* Quasiparticle liquid in the highly overdoped $Bi_2Sr_2CaCu_2O_{8+\delta}$. *Phys. Rev. Lett.* **88**, 167006 (2002).
13. Tyler, A. W. *An Investigation into the Magnetotransport Properties of Layered Superconducting Perovskites.* Ph.D. thesis, Univ. Cambridge (1997).
14. Abdel-Jawad, M. *et al.* Anisotropic scattering and anomalous normal state transport in a high temperature superconductor. *Nature Phys.* **2**, 821–825 (2006).
15. Mackenzie, A. P. *et al.* Calculation of thermodynamic and transport properties of $Sr_2RuO_4$ at low temperatures using known Fermi surface parameters. *Physica C* **263**, 510–515 (1996).
16. Loram, J. W. *et al.* The electronic specific heat of cuprate superconductors. *Physica C* **235–240**, 134–137 (1994).
17. Alexandrov, A. S. Theory of quantum magneto-oscillations in underdoped cuprate superconductors. *J. Phys. Condens. Matter* **20**, 192202 (2008).
18. Proust, C., Boaknin, E., Hill, R. W., Taillefer, L. & Mackenzie, A. P. Heat transport in a strongly overdoped cuprate: Fermi liquid and a pure $d$-wave BCS superconductor. *Phys. Rev. Lett.* **89**, 147003 (2002).
19. Dell'Anna, L. & Metzner, W. Electrical resistivity near Pomeranchuk instability in two dimensions. *Phys. Rev. Lett.* **98**, 136402 (2007).

20. Zhu, L., Aji, V., Shekhter, A. & Varma, C. M. Universality of single-particle spectra of cuprate superconductors. *Phys. Rev. Lett.* **100,** 057001 (2008).
21. Ossadnik, M., Honerkamp, C., Rice, T. M. & Sigrist, M. Breakdown of Landau theory in overdoped cuprates near the onset of superconductivity. Preprint at ⟨http://arXiv.org/abs/0805.3489⟩ (2008).
22. Wasserman, A., Springford, M. & Han, F. The de Haas-van Alphen effect in a marginal Fermi liquid. *J. Phys. Condens. Matter* **3,** 5335–5339 (1991).
23. Wasserman, A. & Springford, M. The influence of many-body interactions on the de Haas-van Alphen effect. *Adv. Phys.* **45,** 471–503 (1996).
24. McCollam, A., Julian, S. R., Rourke, P. M. C., Aoki, D. & Flouquet, J. Anomalous de Haas-van Alphen oscillations in $CeCoIn_5$. *Phys. Rev. Lett.* **94,** 186401 (2005).
25. Tallon, J. L. & Loram, J. W. The doping dependence of $T^*$ — what is the true high-$T_c$ phase diagram? *Physica C* **349,** 53–68 (2001).
26. Lin, J. & Millis, A. J. Theory of low-temperature Hall effect in electron-doped cuprates. *Phys. Rev. B* **72,** 214506 (2005).
27. Chakravarty, S. *et al.* Hidden order in the cuprates. *Phys. Rev. B* **63,** 094503 (2001).
28. Millis, A. J. & Norman, M. R. Antiphase stripe order as the origin of electron pockets observed in 1/8-hole-doped cuprates. *Phys. Rev. B* **76,** 220503 (2007).
29. Schoenberg, D. *Magnetic Oscillations in Metals* (Cambridge Univ. Press, 1984).
30. Bergemann, C., Mackenzie, A. P., Julian, S. R., Forsythe, D. & Ohmichi, E. Quasi-two-dimensional Fermi-liquid properties of the unconventional superconductor $Sr_2RuO_4$. *Adv. Phys.* **52,** 639–725 (2003).

**Acknowledgements** We acknowledge technical and scientific assistance from A. Audouard, M. Nardone, N. Shannon and D. C. Sinclair. This work was supported by EPSRC, LNCMP, the French ANR IceNET and EuroMagNET.

**Author Contributions** The crystals were grown by A.P.M. and screened by M.M.J.F. and N.E.H. The experiments were carried out by B.V., A.C., R.A.C., C.P., C.J., D.V. and N.E.H., and the analysis performed by B.V., A.C., M.M.J.F., C.P. and N.E.H.

**Author Information** Reprints and permissions information is available at www.nature.com/reprints. Correspondence and requests for materials should be addressed to N.E.H. (n.e.hussey@bristol.ac.uk).